

**Line parameters for the 01111-00001 band of $^{12}\text{C}^{16}\text{O}^{18}\text{O}$ from SOIR measurements of the
Venus atmosphere**

V. Wilquet* (1), A. Mahieux (1), A.C. Vandaele (1),
V.I. Perevalov (2), S.A. Tashkun (2),
A. Fedorova (3), O. Korablev (3),
F. Montmessin (4, 5), R.Dahoo (4, 5), J.-L. Bertaux (4, 5)

(1) Belgian Institute for Space Aeronomy, 3 av. Circulaire, B-1180 Brussels, Belgium.

(2) Institute of Atmospheric Optics, Akademicheskii av., 1, 634055, Tomsk, Russia.

(3) Space Research Institute (IKI), 84/32 Profsoyuznaya, 117810 Moscow, Russia

(4) Service d'Aéronomie du CNRS, BP3, 91371, Verrières-le-Buisson, France; Université Pierre et Marie Curie, Paris.

(5) Institut Pierre Simon Laplace, Université de Versailles-Saint-Quentin, 78 Saint Quentin en Yvelines, France.

Keywords : Echelle spectrometer, Venus, CO₂ isotopologue, spectroscopy, CDSO, Hitran

Number of Figures: 4

Number of Tables: 1

* corresponding author : valerie.wilquet@aeronomie.be

Abstract:

CO₂ is the major constituent of the atmosphere of Venus. Absorption lines due to its ¹²C¹⁶O¹⁸O isotopologue have been observed for the first time in Venus spectra in the 2930-3015 cm⁻¹ spectral region, where the HITRAN data base do not contain any line from this isotopologue. The measurements were performed by the SOIR instrument, which is part of the SPICAV/SOIR instrument on board the Venus Express mission of ESA. SOIR was measuring the atmospheric transmission of the upper atmosphere of Venus ($z > 70$ km) by performing a solar occultation experiment, therefore using the atmosphere as a gigantic absorption cell. The identification of this newly observed band was first made recently from Mars atmosphere observations by US colleagues. We have made independent theoretical calculations of the positions of the lines of this new 01111-00001 absorption band, which coincide perfectly with the positions of the observed lines. Assuming an oxygen isotopic ratio similar to the one measured previously in the lower atmosphere of Venus, the line strengths of each observed line are deduced and listed.

1. Introduction

CO₂ is the main component of the atmosphere of Venus, where it represents most of its composition (96.5 %). The first measurements of the atmospheric composition of Venus atmosphere was made by Adams and Dunham [1] using the 100-inch reflector at Mount Wilson. They discovered three bands that they tentatively attributed to CO₂. By 1967 spectroscopic studies performed from Earth clearly identified CO₂ [2]. It also became suspected at that time that CO₂ should be considered as a major or even as the dominant constituent of the Venus atmosphere. In the years 1967-1977, deep-space probes and sounding rockets provided major new discoveries and refinement of the CO₂ observations. By the end of 1977, CO₂ was clearly established as the dominant gas with a mixing ratio larger than 93 % [3]. Starting in December 1978, the Pioneer Venus and Venera 11 and 12 spacecraft performed in situ and remote measurements of the composition of the atmosphere of Venus. They relied on sophisticated mass spectrometers, gas chromatographs, optical spectrometers, ion and EUV mass spectrometers, probing the lower layers as well as the upper region of the atmosphere. They performed comprehensive measurements of the density and composition of the atmosphere including their temporal and spatial variations.

Isotope abundances have been determined in the Venus atmosphere using either earth-based near-infrared spectroscopy or in situ mass spectrometry. Kuiper [4] observed in 1948 structures around 1.47 μm that could be attributed to the ¹³C₂O isotopologue, but the resolution of his spectrum was not sufficient to fully resolve the band. In 1962 Kuiper [5] recorded some 40 absorption bands in the 1.0-2.5 μm spectral region belonging to ¹³C¹⁶O₂ and ¹²C¹⁶O¹⁸O. From those measurements it was found that the ¹³C/¹²C and ¹⁸O/¹⁶O ratios were very similar to those on Earth. Connes and Connes [6] analysed ground-based spectra obtained using a Michelson interferometer and discovered structures due to ¹²C¹⁶O¹⁷O. Mass spectrometric measurements were performed by instruments on board the Pioneer Venus Large Probe and the Venera 11 and 12 lander spacecraft. The Pioneer Venus mass spectrometer [7, 8] found the following values ¹⁸O/¹⁶O = (2.0±0.1)×10⁻³ and ¹³C/¹²C ≤ 1.19×10⁻². The Venera 11 and 12 instruments yielded ¹³C/¹²C = (1.12±0.02)×10⁻². Wilson et al. [9] measured absorption lines in the Venus spectrum at 115 GHz (¹²CO) and at 110 GHz (¹³CO) and found ¹³C/¹²C

= $1/(85 \pm 15)$. Recently, Bézard et al [10] confirmed that the isotopic ratios were very similar to those on Earth. They obtained values of $1/(86 \pm 12)$ and $1/(500 \pm 80)$ for $^{13}\text{C}/^{12}\text{C}$ and $^{18}\text{O}/^{16}\text{O}$ respectively.

SOIR [11, 12] is part of the SPICAV instrument on board Venus Express. It is an Echelle spectrometer combined to an AOT (Acousto-Optical Tunable) Filter used for the order selection. This instrument performs solar occultation measurements in the IR region at a spectral resolution of 0.15 cm^{-1} , the highest spectral resolution ever achieved for a planetary mission. The SOIR instrument is a very sensitive instrument, which already has proven its capability to observe the main isotopologues of the water vapour, namely H_2O and HDO [13]. Measurement of different isotopologues of CO_2 is also possible as the investigated spectral region spans 2200 to 4500 cm^{-1} , which encompass several absorption bands. Figure 1 represents the atmospheric transmission due to CO_2 calculated for a solar occultation with a tangent height of 80 km . The relative importance of two of the isotopologues ($^{12}\text{C}^{16}\text{O}^{16}\text{O}$ and $^{12}\text{C}^{16}\text{O}^{18}\text{O}$) is also shown in the Figure. These calculations have been performed using the line parameters reported in the CDS database [14]. This database is devoted to the compilation of known and calculated CO_2 absorption bands. It has been generated using the method of effective operators and is based on the global fitting of spectroscopic parameters to observed data compiled from the literature. As can be inferred from Figure 1, several micro-regions are favourable for the detection of the $^{12}\text{C}^{16}\text{O}^{18}\text{O}$ isotopologue. However, in the Venus spectra, there is an absorption band located around 2982 cm^{-1} , which does not correspond to anything catalogued neither in the HITRAN nor in the CDS databases. Figure 2 shows such spectra obtained by SOIR orbiting around Venus. The feature located at 2982 cm^{-1} looks like a Q branch with R lines at higher and P lines at lower wavenumbers.

In this work, we will show that those lines are due to $^{12}\text{C}^{16}\text{O}^{18}\text{O}$ and correspond to its 01111-00001 absorption band. This band has never been observed before, not even in the laboratory because of its weakness. Line parameters (positions and intensities) are reported for the first time.

2. Measurements

Absorption lines of an unknown absorber were observed in some of the spectra recorded by SOIR. They were located in the 2930-3015 cm^{-1} spectral range, which correspond to four successive orders of diffraction of the instrument [12]. Those spectra were recorded during sunsets and sunrises, and the unknown component was always observed. Each spectrum has been acquired using a 250 ms integration time. In solar occultation mode, as performed by SOIR, all spectra recorded during the actual occultation are ratioed by a reference spectrum which is obtained outside the atmosphere. These transmittances show the characteristic behavior observed on all occultation series measured on Venus, see Figure 2. This set corresponds to setting of the sun. At the beginning of the series, the light path does not cross the atmosphere. No absorption signatures are present and transmittances are equal to unity. As the sun sets, the light path goes deeper and deeper into the atmosphere, and two absorption processes take place: the overall signal decreases due to extinction by aerosols and absorption signatures appear. At the end, the light path crosses the cloud layer situated at an altitude of 60 km above the Venus surface: no light is transmitted anymore. In general, the SOIR spectra contain information on the Venus atmosphere between 65 km and 120 km. Several lines of HCl are present, but other lines are showing up: a Q branch is well recognizable (Fig. 2B) and a series of lines belonging to a P branch (Fig. 2A) and to an R branch (Fig. 2B) are also visible. This band is not reported in databases, like HITRAN or CDS. Other lines are also visible, although some care must be taken in the interpretation. Indeed, the AOTF bandpass slightly exceeds the Free Spectral Range of the spectrometer, thus the diffraction order selected by the AOTF also contains light coming from the four adjacent orders (two longward and two shortward), This artefact may not only induce confusion in the line position, it can also affect the depth of a band and subsequently the deduced quantity of absorber.

3. Line positions

Though the 01111-00001 band has never been observed, the line positions of the hot band 01111-01101, which has the same upper state, have been measured [15, 16]. These measurements enabled us to calculate the rotational structure of the 01111 vibrational state with an uncertainty of about 0.001 cm^{-1} using the effective Hamiltonian approach [17]. The calculated line positions are given in

Table 1, in which the observed values are reported. The difference between the theoretical and measured values ($\Delta\nu$) is also given, the average $|\Delta\nu|$ for all lines observed in the SOIR spectra is 0.03 cm^{-1} , in good agreement with the calculated uncertainty for the line position (0.05 cm^{-1}) [11]. Figure 3 illustrates the very good match between predicted and measured line positions.

4. Line intensities

Unfortunately the effective operator approach [18], which was used to retrieve effective dipole moment parameters from observed intensities does not allow us to calculate intensities of the 01111-00001 band. The reason is that up to now there are no laboratory measured intensities of $^{12}\text{C}^{16}\text{O}^{18}\text{O}$ bands with $\Delta V_1=0$, $\Delta V_2=1$, $\Delta V_3=1$, $\Delta \ddot{y}_2=\pm 1$. That is why this band was absent from the CDSD databank.

Information on the intensity of the $^{12}\text{C}^{16}\text{O}^{18}\text{O}$ lines can be learned from the SOIR spectra.

Simulations of spectra using ASIMUT [19], taking into account the geometry of the solar occultation and calculating the additive effect of 7 orders in total (the centre one plus 6 adjacent ones) were performed using an initial line list, constructed on the theoretical line positions discussed previously and with initial guesses for the intensities chosen to follow a Boltzmann distribution. These simulations calculate the optical density due to CO_2 along the refracted path through the atmosphere, taking into account the temperature and pressure profiles of the atmosphere. The CO_2 a priori density vertical profile is the one of the VIRA model [20] and the commonly chosen value of 1/500 for the $^{16}\text{O}/^{18}\text{O}$ ratio was considered, which is very similar to the one on Earth. Values for the broadening parameters were kept identical for all lines ($\gamma_{\text{CO}_2\text{-CO}_2}=0.08 \text{ cm}^{-1} \text{ atm}^{-1}$ with $n=0.7$) and CO_2 lines were simulated by Voigt line profiles.

Figure 4 shows some results of the simulations. Observed spectra were obtained at an altitude of $\sim 80 \text{ km}$, which, according to the VIRA model [20], corresponds to a T° of 200K. The spectra are coming from various diffraction orders, hence corresponding to different wavenumber ranges, and are compared with their associated simulations using the new line list, which is available as supplementary material (Table 1).

The line position and intensities obtained in the present work are reported for the first time.

However, this new absorption feature was also recently observed by a US team from the Earth's

ground in the spectrum of solar light reflected by the ground of Mars [21]. In a recent paper of Toth et al. [22], investigating the absorption properties of CO₂ isotopologues between 2200 and 7000 cm⁻¹, there was no mention of the feature observed at 2982 cm⁻¹. Their most sensitive runs (runs 155.9 and 155.12, see experimental conditions, their Table 2) for the detection of this band corresponded to a slant value of N(628) of 3.3 10²⁰ mol/cm², and according to our values, it would have given rise to an absorption of 1.2 10⁻³, averaged over 2 cm⁻¹ [23]. However, given their much higher resolution (than SOIR) of 0.01 cm⁻¹, deeper absorption features could have been present in their spectra. Their S/N was 200-250 for these runs, and probably the absorption was marginally detectable and went unnoticed.

5. Conclusions

The 01111-00001 absorption band of ¹²C¹⁶O¹⁸O has been observed for the first time using solar occultation measurements of the atmosphere of Venus, where CO₂ is the major constituent. Combining theoretical investigations and the analysis of the Venus spectra, a new line list has been build. This list reports line position and attribution for 194 lines. For 149 of those lines, intensities could be derived from the Venus spectra. Not only will the SOIR instrument improve our knowledge of the Venusian atmosphere, by measuring routinely important species as CO₂, H₂O, HDO, HCl, HF, and CO, but it has also proven its capacity to deliver new results at the spectroscopic level. In near future, we will investigate the entire spectral range of the instrument for the possibility to improve the quality of the CO₂ spectroscopic database.

Acknowledgments

The research program was supported by the Belgian Federal Science Policy Office and the European Space Agency (ESA – PRODEX program – contract C 90268). VIP and SAT acknowledge the support from the RFBR-CNRS PICS grant 05-05-22001.

References

1. Adams, W.S. and T. Dunham, Absorption bands in the infrared spectrum of Venus, *Publ. Astron. Soc. Pacific.*, 44, 243-247, 1932.
2. Connes, P., et al., Traces of HCl and HF in the atmosphere of Venus, *Astrophys. J.*, 147, 1230-1237, 1967.
3. Vinogradov, A., et al., *Chemical composition of the Venus atmosphere*, in *Planetary Atmospheres*, C. Sagan, T. Owen, and H. Smith, Editors. 1971, Springer Verlag: New York. p. 3-16.
4. Kuiper, G., *Survey of planetary atmospheres*, in *The atmospheres of the Earth and Planets*, G. Kuiper, Editor. 1949, Univ. Chicago Press: Chicago. p. 306-405.
5. Kuiper, G., Infrared spectra of stars and planets. I. Photometry of the infrared spectrum of Venus, 1-2.5 microns, *Comm. Lunar Planet. Lab.*, 1, 83-117, 1962.
6. Connes, J. and P. Connes, Near-infrared planetary spectra by Fourier spectroscopy. I. Instruments and results, *J. Opt. Soc. Amer.*, 56, 896-910, 1966.
7. Hoffman, J., et al., Venus lower atmospheric composition: Preliminary results from Pioneer Venus, *Science*, 203, 800-802, 1979.
8. Hoffman, J., et al., Composition of the Venus lower atmosphere from the Pioneer Venus mass spectrometer, *J. Geophys. Res.*, 85, 7882-7890, 1980.
9. Wilson, W., et al., Venus. I. Carbon monoxide distribution and molecular-line searches, *Icarus*, 45, 624-637, 1981.
10. Bézard, B., et al., The $^{12}\text{C}/^{13}\text{C}$ and $^{16}\text{O}/^{18}\text{O}$ ratios in the atmosphere of Venus from high-resolution 10- μm spectroscopy, *Icarus*, 72(3), 623-634, 1987.
11. Mahieux, A., et al., In-Flight performances of SPICAV SOIR on board Venus Express, AO, (submitted), 2007.
12. Nevejans, D., Compact high-resolution space-borne echelle grating spectrometer with AOTF based order sorting for the infrared domain from 2.2 to 4.3 micrometer, AO, 2006.
13. Bertaux, J.-L., et al., A warm layer in Venus' cryosphere and high altitude measurements of HF, HCl, H₂O and HDO, *Nature*, (in press), 2007.
14. Tashkun, S.A., et al., CDSD-1000, the high-temperature carbon dioxide spectroscopic databank, *JQSRT*, 82, 165-196, 2003.
15. Esplin, M.P., et al., Carbon dioxide line positions in the 2.8 and 4.3 micron regions at 800 Kelvin, AFGL-TR-86-0046, 1986.
16. Bailly, D., thesis, University Pierre et Marie Curie, Paris, 1983.
17. Tashkun, S.A., et al., Global fitting of $^{12}\text{C}^{16}\text{O}_2$ vibrational-rotational line positions using the effective Hamiltonian approach, *JQSRT*, 60, 785-801, 1998.
18. Tashkun, S.A., et al., Global fit of $^{12}\text{C}^{16}\text{O}_2$ vibrational-rotational line intensities using the effective operator approach, *JQSRT*, 62, 571-598, 1999.
19. Vandaele, A.C., et al., Modeling and retrieval of atmospheric spectra using ASIMUT, *JQSRT*, (submitted in the same special issue), 2007.
20. Keating, G.M., Bertaux, J.L., Bougher, S.W., Cravens, T.E., Dickinson, R.E., Hedin, A.E., V.A. Krasnopolsky, A.F. Nagy, J.Y. Nicholson, L.J. Paxton, U. Von Zahn VIRA (Venus International Reference Atmosphere) Models of Venus Neutral Upper Atmosphere : Structure and Composition, eds : A.J. Kliore, V.I. Moroz, and G.M. Keating, *Advan. Space Research*, 5, n° 11, pp. 117-171 (1985)
21. Villanueva, G., et al., Identification of a New Band System of Isotopic CO₂ near 3.3 μm : Implications for Remote Sensing of Biomarker Gases on Mars, *Icarus*, (submitted), 2007.
22. Toth, R.A., et al., Line positions and strengths of $^{16}\text{O}^{12}\text{C}^{18}\text{O}$, $^{18}\text{O}^{12}\text{C}^{18}\text{O}$ and $^{17}\text{O}^{12}\text{C}^{18}\text{O}$ between 2200 and 7000 cm^{-1} , *JMS*, 243, 43-61, 2007.
23. Bertaux, J.-L., et al., First Observation of 628 CO₂ isotopologue band at 3.3 μm in the atmosphere of Venus by solar occultation from Venus Express, *Icarus*((submitted)), 2007.

Figure captions

Figure 1: Transmission due to CO₂ calculated for a solar occultation through the Venus atmosphere corresponding to a tangent height of 80 km. (A) All isotopologues of CO₂, (B) the main isotopologue ¹²C¹⁶O¹⁶O, (C) ¹²C¹⁶O¹⁸O. Line parameters are from the CDSD-1000 database. The box delimits the wavenumber range for diffraction orders 132 and 133, and the thick line indicates the wavenumber range of the 01111-00001 band.

Figure 2: A series of transmittances obtained during one occultation recorded by SOIR in the 2950-2997 cm⁻¹ spectral domain. (A) Diffraction order 132: the regularly spaced P lines are visible, as well as a Q branch due to light pollution from the adjacent order. (B) Diffraction order 133: the Q branch is clearly visible, as well as a series of R lines. In addition to those lines, some lines due to HCl are also present. They are marked by an asterisk.

Figure 3: Comparison between calculated and measured line positions. The actual SOIR transmittance is in blue while the black vertical lines of arbitrary length represent the theoretical values for the line positions. (A) Diffraction order 132. (B) Diffraction order 133.

Figure 4: Results of determination of the line intensities at 200K. Observed (blue line) and simulated (red line) spectra of HCl and of the CO₂ band or both HCl and CO₂ in 2 different orders. Beneath the latter, a panel gives the residual transmittance. (A) Diffraction order 132. (B) Diffraction order 133.

Table captions

Table 1: Line positions and intensities found in this work. Predicted and measured positions are given, as well as the difference between them ($\Delta\nu$) and the absolute line intensity derived from simulations with ASIMUT of SOIR spectra obtained at 200K. ‘no’ stands for lines that could not be detected in the spectra and ‘undef’ for unresolved lines of the Q branch.

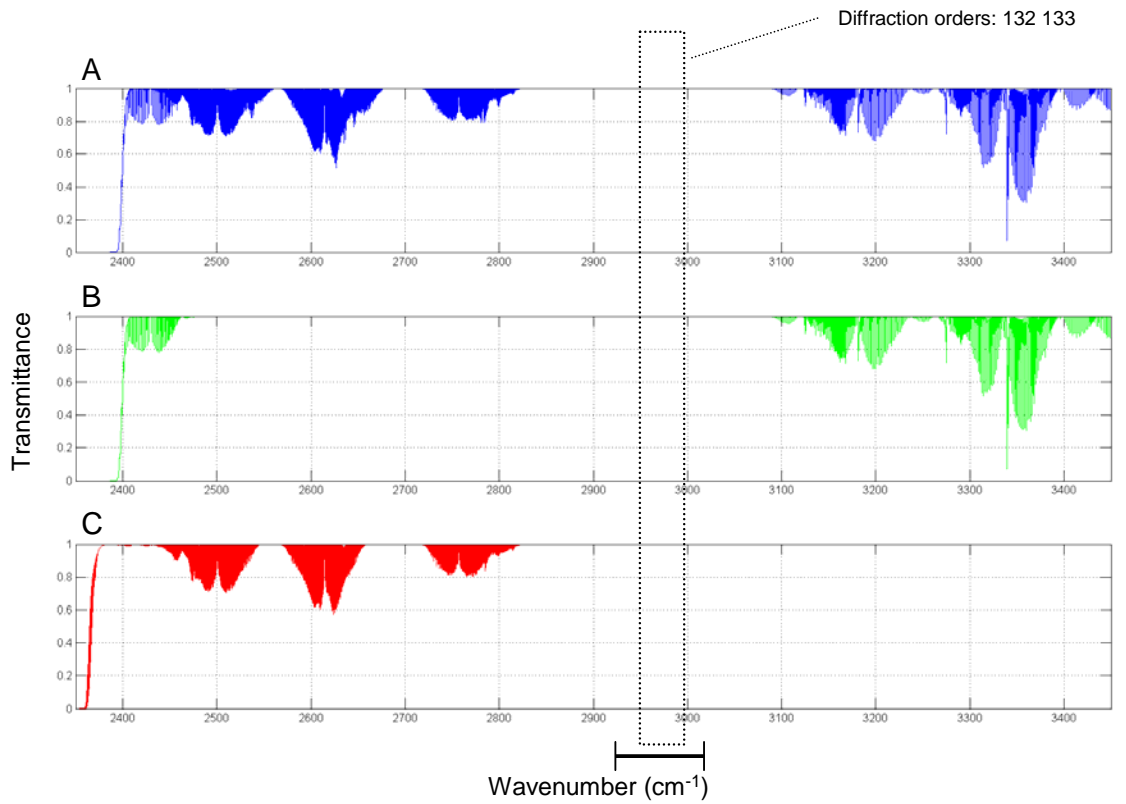


Figure 1: Transmission due to CO₂ calculated for a solar occultation through the Venus atmosphere corresponding to a tangent height of 80 km. (A) All isotopologues of CO₂, (B) the main isotopologue ¹²C¹⁶O¹⁶O, (C) ¹²C¹⁶O¹⁸O. Line parameters are from the CDSD-1000 database. The box delimits the wavenumber range for diffraction orders 132 and 133, and the thick line indicates the wavenumber range of the 01111-00001 band.

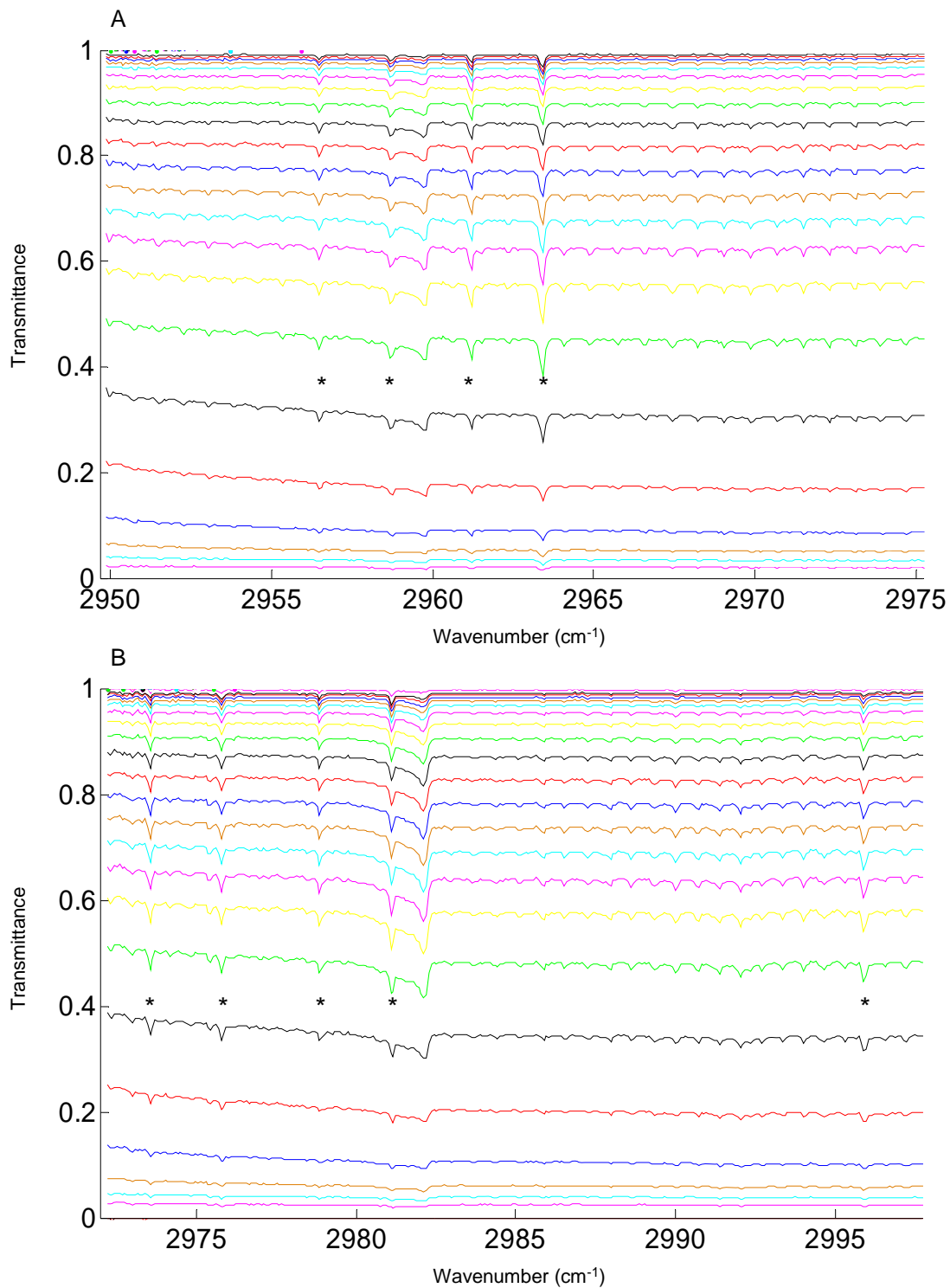


Figure 2: A series of transmittances obtained during one occultation recorded by SOIR in the 2950-2997 cm⁻¹ spectral domain. (A) Diffraction order 132: the regularly spaced P lines are visible, as well as a Q branch due to light pollution from the adjacent order. (B) Diffraction order 133: the Q branch is clearly visible, as well as a series of R lines. In addition to those lines, some lines due to HCl are also present. They are marked by an asterisk.

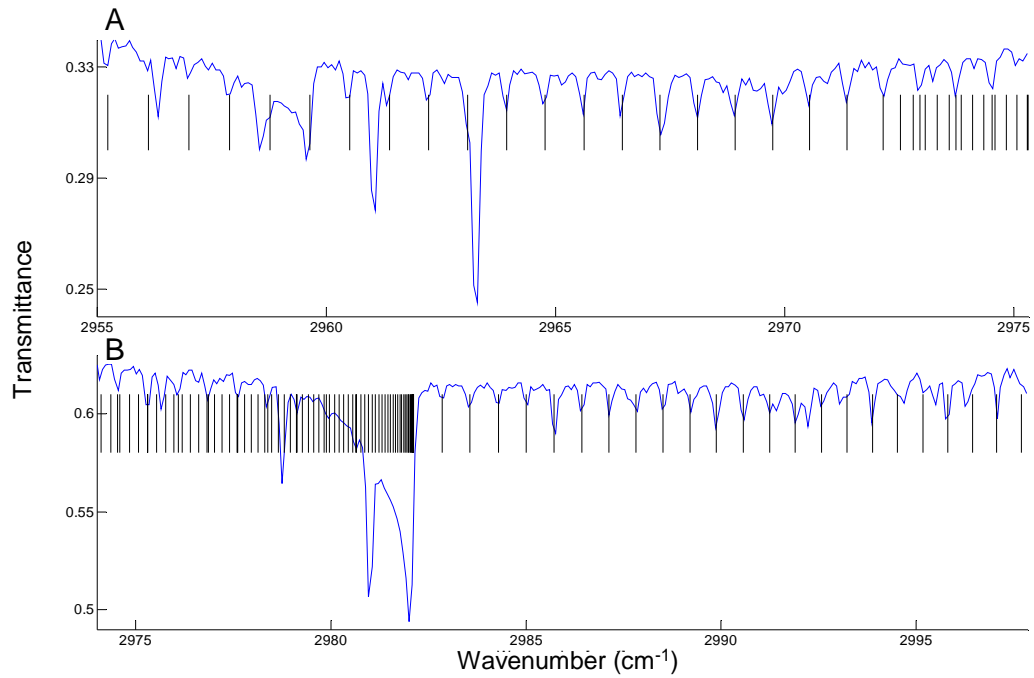


Figure 3: Comparison between calculated and measured line positions. The actual SOIR transmittance is in blue while the black vertical lines of arbitrary length represent the theoretical values for the line positions. (A) Diffraction order 132. (B) Diffraction order 133.

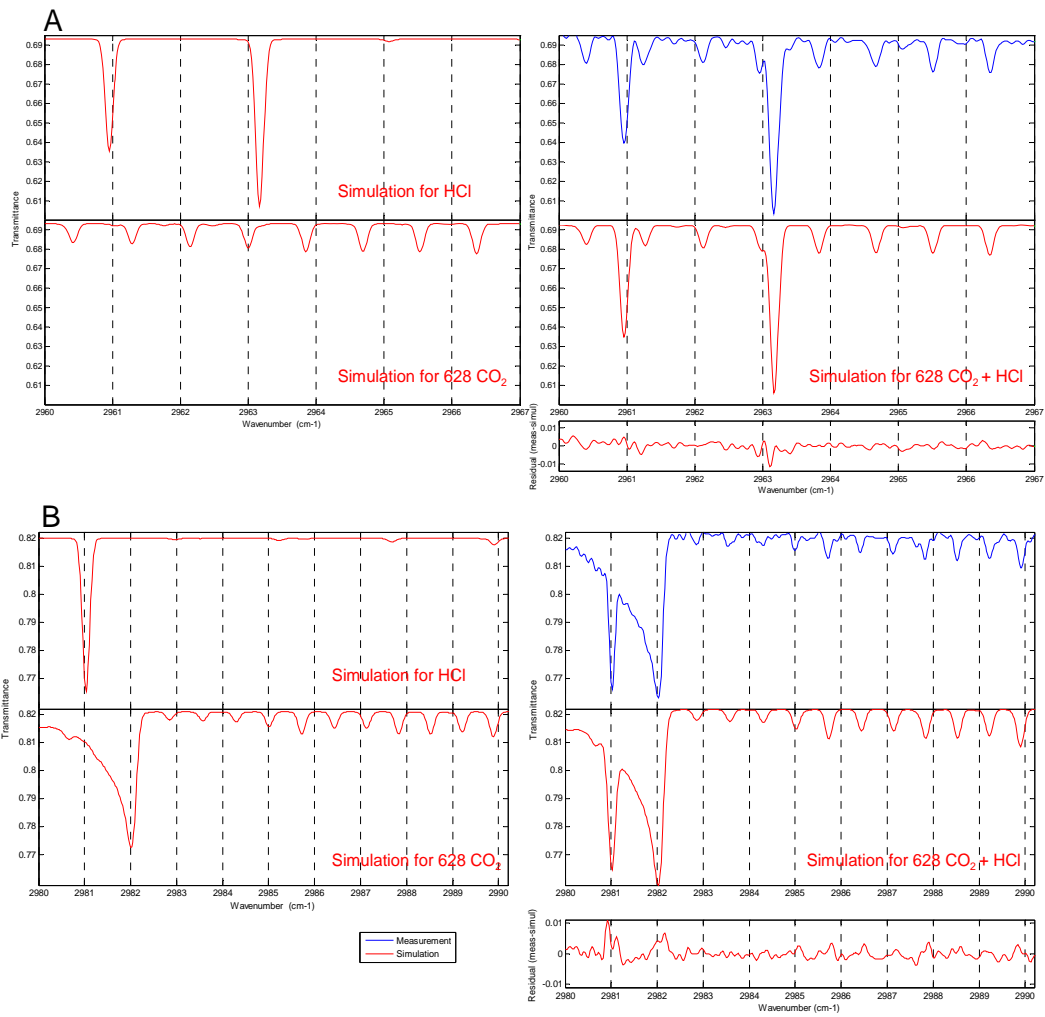


Figure 4: Results of determination of the line intensities at 200K. Observed (blue line) and simulated (red line) spectra of HCl and of the CO₂ band or both HCl and CO₂ in 2 different orders. Beneath the latter, a panel gives the residual transmittance. (A) Diffraction order 132. (B) Diffraction order 133.

line		ν (calculated) cm^{-1}	ν (measured) cm^{-1}	$\Delta\nu$ cm^{-1}	Intensity $\text{cm}^{-1}/(\text{molec.cm}^2)$
P	2	2980.634	2980.67	0.04	3.75E-26
P	3	2979.888	2979.88	-0.01	3.75E-26
P	4	2979.137	2979.17	0.03	3.75E-26
P	5	2978.381	2978.38	0.00	6.25E-26
P	6	2977.620	2977.66	0.04	1.00E-25
P	7	2976.854	2976.87	0.02	8.75E-26
P	8	2976.084	2976.07	-0.01	8.75E-26
P	9	2975.308	2975.35	0.04	1.13E-25
P	10	2974.528	2974.53	0.00	1.75E-25
P	11	2973.742	2973.72	-0.02	2.06E-25
P	12	2972.952	2972.91	-0.04	2.06E-25
P	13	2972.157	2972.16	0.00	2.06E-25
P	14	2971.357	2971.34	-0.02	2.31E-25
P	15	2970.552	2970.53	-0.02	2.25E-25
P	16	2969.743	2969.70	-0.04	2.31E-25
P	17	2968.928	2968.90	-0.03	1.81E-25
P	18	2968.109	2968.09	-0.02	1.81E-25
P	19	2967.285	2967.30	0.02	1.96E-25
P	20	2966.456	2966.42	-0.04	1.88E-25
P	21	2965.622	2965.60	-0.02	1.75E-25
P	22	2964.783	2964.73	-0.05	1.81E-25
P	23	2963.939	2963.93	-0.01	1.80E-25
P	24	2963.091	2963.06	-0.03	1.74E-25
P	25	2962.237	2962.20	-0.04	1.68E-25
P	26	2961.379	2961.32	-0.06	1.60E-25
P	27	2960.516	2960.48	-0.04	1.63E-25
P	28	2959.648	2959.65	0.00	1.44E-25
P	29	2958.775	2958.78	0.00	1.26E-25
P	30	2957.898	2957.87	-0.03	1.17E-25
P	31	2957.015	2956.98	-0.04	1.09E-25
P	32	2956.128	2956.10	-0.03	1.00E-25
P	33	2955.236	2955.22	-0.02	9.21E-26
P	34	2954.339	2954.37	0.03	8.75E-26
P	35	2953.437	2953.42	-0.02	7.66E-26
P	36	2952.531	2952.50	-0.03	6.94E-26
P	37	2951.619	2951.62	0.00	6.26E-26
P	38	2950.703	2950.74	0.04	5.63E-26
P	39	2949.782	2949.79	0.01	5.00E-26
P	40	2948.856	2948.82	-0.04	4.38E-26
P	41	2947.926	2947.97	0.04	3.63E-26
P	42	2946.990	2947.00	0.01	2.88E-26
P	43	2946.050	2946.10	0.05	2.13E-26
P	44	2945.105	2945.09	-0.01	1.38E-26
P	45	2944.155	2944.16	0.01	5.00E-27
P	46	2943.200	2943.26	0.06	4.13E-27
P	47	2942.241	2942.25	0.01	3.25E-27
P	48	2941.276	2941.30	0.02	2.38E-27
P	49	2940.307	2940.36	0.05	1.50E-27
P	50	2939.333	2939.28	-0.05	5.00E-28
P	51	2938.355	2938.33	-0.02	4.00E-28
P	52	2937.371	2937.38	0.01	3.00E-28
P	53	2936.383	2936.42	0.04	2.00E-28

line		ν (calculated) cm ⁻¹	ν (measured) cm ⁻¹	$\Delta\nu$ cm ⁻¹	Intensity cm ⁻¹ /(molec.cm ²)
P	54	2935.389	2935.41	0.02	1.00E-28
P	55	2934.392	2934.39	0.00	1.25E-29
P	56	2933.389	2933.43	0.04	1.00E-29
P	57	2932.381	2932.36	0.02	1.00E-29
P	58	2931.369	2931.37	0.00	1.00E-30
P	59	2930.352	2930.33	0.02	1.00E-30
P	60	2929.330	no		
P	61	2928.303	no		
P	62	2927.272	no		
P	63	2926.235	no		
P	64	2925.194	no		
P	65	2924.148	no		
P	66	2923.098	no		
P	67	2922.042	no		
P	68	2920.982	no		
P	69	2919.917	no		
P	70	2918.847	no		
P	71	2917.773	no		
Q	1	2982.108	undef		3.75E-26
Q	2	2982.100	undef		6.25E-26
Q	3	2982.089	undef		8.75E-26
Q	4	2982.073	undef		1.13E-25
Q	5	2982.054	undef		1.75E-25
Q	6	2982.031	undef		1.88E-25
Q	7	2982.004	undef		1.75E-25
Q	8	2981.974	undef		1.75E-25
Q	9	2981.939	undef		1.75E-25
Q	10	2981.901	undef		1.75E-25
Q	11	2981.859	undef		1.88E-25
Q	12	2981.813	2981.83	0.02	1.88E-25
Q	13	2981.763	2981.78	0.02	2.00E-25
Q	14	2981.709	undef		2.00E-25
Q	15	2981.652	2981.67	0.02	2.00E-25
Q	16	2981.590	undef		2.13E-25
Q	17	2981.525	undef		2.13E-25
Q	18	2981.456	2981.46	0.00	2.13E-25
Q	19	2981.383	undef		2.13E-25
Q	20	2981.307	2981.30	-0.01	2.13E-25
Q	21	2981.226	undef		2.13E-25
Q	22	2981.142	undef		1.88E-25
Q	23	2981.053	undef		1.88E-25
Q	24	2980.961	undef		1.88E-25
Q	25	2980.865	undef		1.75E-25
Q	26	2980.765	2980.72	-0.05	1.75E-25
Q	27	2980.662	2980.67	0.01	1.75E-25
Q	28	2980.554	undef		1.75E-25
Q	29	2980.443	2980.40	-0.04	1.75E-25
Q	30	2980.328	undef		1.75E-25
Q	31	2980.209	2980.23	0.02	1.75E-25
Q	32	2980.086	2980.12	0.03	1.75E-25
Q	33	2979.959	2980.02	0.06	1.75E-25
Q	34	2979.828	2979.85	0.02	1.75E-25

line		ν (calculated) cm ⁻¹	ν (measured) cm ⁻¹	$\Delta\nu$ cm ⁻¹	Intensity cm ⁻¹ /(molec.cm ²)
Q	35	2979.694	2979.72	0.03	1.75E-25
Q	36	2979.555	2979.56	0.00	1.75E-25
Q	37	2979.413	2979.41	0.00	1.75E-25
Q	38	2979.267	2979.25	-0.02	1.75E-25
Q	39	2979.117	2979.16	0.04	1.75E-25
Q	40	2978.963	2978.96	0.00	1.50E-27
Q	41	2978.805	2978.77	-0.04	5.00E-26
Q	42	2978.644	2978.60	-0.04	4.00E-26
Q	43	2978.478	2978.46	-0.02	6.25E-25
Q	44	2978.309	no		6.25E-25
Q	45	2978.136	2978.14	0.00	1.00E-26
Q	46	2977.959	2978.02	0.06	1.25E-28
Q	47	2977.778	2977.75	-0.03	2.38E-27
Q	48	2977.593	2977.53	-0.06	1.50E-25
Q	49	2977.404	2977.35	-0.05	5.00E-28
Q	50	2977.211	2977.22	0.01	4.00E-28
Q	51	2977.015	2977.00	-0.01	3.00E-28
Q	52	2976.814	2976.86	0.05	2.00E-28
Q	53	2976.610	2976.63	0.02	1.00E-28
Q	54	2976.401	2976.43	0.03	1.25E-29
Q	55	2976.189	2976.15	-0.04	1.38E-26
Q	56	2975.973	no		5.00E-27
Q	57	2975.753	2975.75	0.00	4.13E-27
Q	58	2975.529	no		3.25E-27
Q	59	2975.301	2975.27	-0.03	2.38E-27
Q	60	2975.069	2975.11	0.04	1.50E-27
Q	61	2974.834	2974.81	-0.02	5.00E-28
Q	62	2974.594	2974.56	-0.03	4.00E-28
Q	63	2974.350	2974.36	0.01	3.00E-28
Q	64	2974.103	2974.16	0.06	2.00E-28
Q	65	2973.851	2973.83	-0.02	1.00E-28
Q	66	2973.596	no		1.25E-29
Q	67	2973.337	no		1.00E-29
Q	68	2973.073	2973.11	0.04	1.00E-29
Q	69	2972.806	2972.80	-0.01	8.00E-30
Q	70	2972.535	2972.57	0.04	8.00E-30
R	0	2982.843	2982.89	0.05	5.00E-26
R	1	2983.570	2983.55	-0.02	5.63E-26
R	2	2984.291	2984.31	0.02	6.20E-26
R	3	2985.008	2985.02	0.01	9.00E-26
R	4	2985.720	2985.75	0.03	1.35E-25
R	5	2986.427	2986.42	-0.01	1.00E-25
R	6	2987.129	2987.15	0.02	1.00E-25
R	7	2987.826	2987.85	0.02	1.40E-25
R	8	2988.518	2988.51	-0.01	1.44E-25
R	9	2989.205	2989.23	0.02	1.30E-25
R	10	2989.887	2989.89	0.00	1.70E-25
R	11	2990.565	2990.62	0.06	1.70E-25
R	12	2991.237	2991.28	0.04	1.88E-25
R	13	2991.904	2991.93	0.03	2.44E-25
R	14	2992.567	2992.60	0.03	1.63E-25
R	15	2993.224	2993.25	0.03	1.50E-25

line	ν (calculated) cm ⁻¹	ν (measured) cm ⁻¹	$\Delta\nu$ cm ⁻¹	Intensity cm ⁻¹ /(molec.cm ²)	
R	16	2993.877	2993.92	0.04	1.88E-25
R	17	2994.524	2994.60	0.08	1.96E-25
R	18	2995.167	2995.16	-0.01	1.94E-25
R	19	2995.805	2995.78	-0.02	1.90E-25
R	20	2996.437	2996.42	-0.02	1.86E-25
R	21	2997.065	2997.07	0.01	1.80E-25
R	22	2997.688	2997.70	0.01	1.74E-25
R	23	2998.305	2998.32	0.01	1.68E-25
R	24	2998.918	2998.91	-0.01	1.60E-25
R	25	2999.526	2999.53	0.00	1.51E-25
R	26	3000.129	3000.10	-0.03	1.44E-25
R	27	3000.726	3000.74	0.01	1.26E-25
R	28	3001.319	3001.30	-0.02	1.17E-25
R	29	3001.907	3001.93	0.02	1.09E-25
R	30	3002.490	3002.43	-0.06	1.00E-25
R	31	3003.067	3003.06	-0.01	9.21E-26
R	32	3003.640	3003.62	-0.02	8.41E-26
R	33	3004.208	3004.19	-0.02	7.66E-26
R	34	3004.771	3004.75	-0.02	6.94E-26
R	35	3005.328	3005.35	0.02	6.26E-26
R	36	3005.881	3005.90	0.02	5.63E-26
R	37	3006.428	3006.38	-0.05	5.00E-26
R	38	3006.971	3007.00	0.03	4.38E-26
R	39	3007.509	3007.48	-0.03	3.63E-26
R	40	3008.041	3008.07	0.03	2.88E-26
R	41	3008.568	3008.61	0.04	2.13E-26
R	42	3009.091	3009.10	0.01	1.38E-26
R	43	3009.608	3009.59	-0.02	5.00E-27
R	44	3010.120	3010.10	-0.02	4.13E-27
R	45	3010.628	3010.59	-0.04	3.25E-27
R	46	3011.130	no		
R	47	3011.627	no		
R	48	3012.119	3012.11	-0.01	
R	49	3012.605	no		
R	50	3013.087	3013.07	-0.02	
R	51	3013.564	no		
R	52	3014.035	no		
R	53	3014.502	no		

Table 1: Line intensities found in this work. Predicted and measured positions are given, as well as the difference between them ($\Delta\nu$) and the absolute line intensity derived from simulations with ASIMUT of SOIR spectra obtained at 200K. 'no' stands for lines that could not be detected in the spectra and 'undef' for unresolved lines of the Q branch.